Mutually opposing activity of PIN7 splicing isoforms is required for auxin-mediated tropic responses in *Arabidopsis thaliana*

Ivan Kashkan[1,2], Mónika Hrtyan[2], Roberta Filepová[1], Zuzana Vondráková[1], Jan Hejátko[2], Sibu Simon[1], Debbie Rombaut[3,4], Thomas B. Jacobs[3,4], Mikko J. Frilander[5], Jiří Friml[6], Jan Petrášek[1], Kamil Růžička[1,2,7,*]

[1]*Laboratory of Hormonal Regulations in Plants, Institute of Experimental Botany, Czech Academy of Sciences, 16502 Prague, Czech Republic*

[2]*Functional Genomics and Proteomics of Plants, Central European Institute of Technology and National Centre for Biomolecular Research, Masaryk University, 62500 Brno, Czech Republic*

[3]*Department of Plant Biotechnology and Bioinformatics, Ghent University, 9052 Ghent, Belgium*

[4]*VIB Center for Plant Systems Biology, 9052 Ghent, Belgium*

[5]*Institute of Biotechnology, University of Helsinki, 00014 University of Helsinki, Finland*

[6]*Institute of Science and Technology (IST Austria), 3400 Klosterneuburg, Austria*

[7]*Lead Contact*

[*]Correspondence: kamil.ruzicka@ueb.cas.cz

SUMMARY

Advanced transcriptome sequencing has revealed that the majority of eukaryotic genes undergo alternative splicing (AS). Nonetheless, limited effort has been dedicated to investigating the functional relevance of particular splicing events, even those in the key developmental and hormonal regulators. Here we reveal, in the plant model *Arabidopsis thaliana*, that the *PIN7* gene, which encodes a polarly localized transporter for the phytohormone auxin, produces two evolutionarily conserved transcripts. These isoforms PIN7a and PIN7b, differing in a 4 amino acid motif, are present at nearly equal levels in most cells, except some early developing tissues where the expression of PIN7b is moderately prevalent. Both proteins also transport auxin with similar capacity and directionality. However, only *PIN7a* but not *PIN7b* cDNA rescues the phenotypes associated with the *pin7* knock-out mutation, consistent with their differences in the subcellular trafficking and dynamics at the plasma membrane. Further phenotypic analyses suggested a joint, mutually opposing activity of both isoforms as being required for correct seedling apical hook formation and auxin-mediated tropic responses. These results establish alternative splicing of the PIN family as an evolutionary conserved, functionally relevant mechanism, taking part in the auxin-mediated plant development.

KEYWORDS

Auxin, auxin transport, PINs, alternative splicing, plant development, RNA processing, tropic responses

INTRODUCTION

Auxin is an essential phytohormone, which plays a role in nearly all aspects of plant development. To flexibly adapt to rapidly changing environmental cues, directional auxin transport represents a highly dynamic means for triggering downstream morphogenetic processes. PIN FORMED (PIN) auxin efflux carriers are among the key regulators in this respect. Many efforts in the past years uncovered several mechanisms operating transcriptionally or post-translationally on the capacity and directionality of PIN-mediated transport. However, little progress has been made in exploring the contribution of post-transcriptional regulation (Adamowski and Friml, 2015; Hrtyan et al., 2015).

Advances in high throughput sequencing have revealed unexpected complexity within eukaryotic transcriptomes by alternative splicing (AS). Although the majority of AS transcripts may be functionally neutral (Darracq and Adams, 2013; Reddy et al., 2013; Tress

et al., 2017; Blencowe, 2017; Mei et al., 2017), several detailed studies have highlighted a plausible role for numerous AS events in physiologically relevant contexts, including those involved in plant developmental and hormonal pathways (Staiger and Brown, 2013; Hrtyan et al., 2015; Shang et al., 2017; Szakonyi and Duque, 2018). Earlier works have described auxin-related defects resulting from the aberrant function of several regulators of AS (Kalyna et al., 2003; Casson et al., 2009; Retzer et al., 2014; Tsugeki et al., 2015; Hrtyan et al., 2015; Bazin et al., 2018). AS changes subcellular localization of the auxin biosynthetic gene *YUCCA 4* (Kriechbaumer et al., 2012) and differential splicing of an exitron (Marquez et al., 2015) inside the *AUXIN RESPONSE FACTOR 8* results in developmental changes of generative organs (Ghelli et al., 2018). AS of the Major Facilitator Superfamily transporter ZIFL1 interferes with auxin transport, influencing the stability of PINs on the plasma membrane (PM) (Remy et al., 2013). These lines of evidence suggest that AS is an important player in auxin-dependent processes. However, no coherent functional model of any auxin-related AS event has been provided so far.

Here, we characterize AS of the *PIN7* gene in *Arabidopsis thaliana*. PIN7 is, together with PIN3 and PIN4, a member of the PIN3 clade of PIN auxin efflux carriers (Bennett et al., 2014), which are required for a broad range of morphogenetic and tropic processes (Adamowski and Friml, 2015). We reveal that AS influences the dynamics of the PIN7 protein on the PM. We also demonstrate that the coordinated action of both splice variants is required for fine-tuning auxin-mediated tropic responses and during apical hook development.

RESULTS

Arabidopsis PIN7 and *PIN4* produce two evolutionarily conserved AS transcripts

Our previous survey (Hrtyan et al., 2015) revealed that several genes involved in auxin-dependent processes undergo AS. Among them, closely related paralogs from the *PIN3* clade of auxin transporters, *PIN4* and *PIN7* (but not *PIN3*), are regulated by the same type of AS (Petrasek et al., 2006; Bennett et al., 2014; Hrtyan et al., 2015). The resulting transcripts, denoted as *a* and *b*, differ in the position of the AS donor site in the first intron (Figure 1A). The differentially spliced region corresponds to a four amino acid motif inside the large internal hydrophilic loop (Ganguly et al., 2014; Nodzyński et al., 2016) of the integral PM transporter (Figure 1A and 1B). We examined the quantities of individual reads spanning the exon junctions in the respective region from the *Arabidopsis* root tip and in several other available transcriptomes from different tissues and organs (Klepikova et al., 2016; Cheng et al., 2017; Ruzicka et al., 2017) (Figures 1C and Supplemental Figure 1A). We found that both

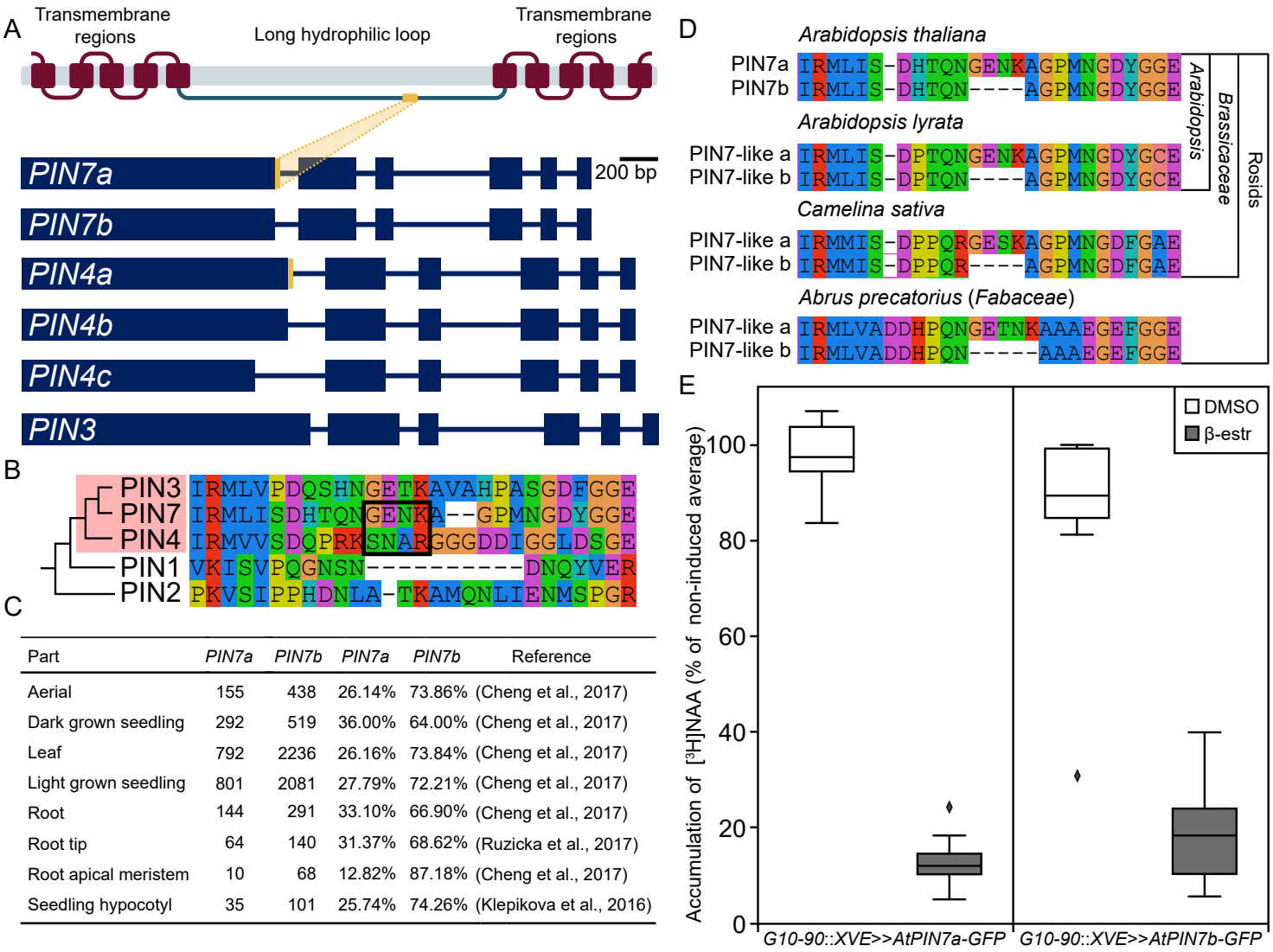

Part	*PIN7a*	*PIN7b*	*PIN7a*	*PIN7b*	Reference
Aerial	155	438	26.14%	73.86%	(Cheng et al., 2017)
Dark grown seedling	292	519	36.00%	64.00%	(Cheng et al., 2017)
Leaf	792	2236	26.16%	73.84%	(Cheng et al., 2017)
Light grown seedling	801	2081	27.79%	72.21%	(Cheng et al., 2017)
Root	144	291	33.10%	66.90%	(Cheng et al., 2017)
Root tip	64	140	31.37%	68.62%	(Ruzicka et al., 2017)
Root apical meristem	10	68	12.82%	87.18%	(Cheng et al., 2017)
Seedling hypocotyl	35	101	25.74%	74.26%	(Klepikova et al., 2016)

Figure 1. Alternative splicing (AS) of the Arabidopsis thaliana PIN7 and PIN4 leads to two evolutionary conserved functional transcripts.

(A) Scheme of coding regions of the PIN3 clade genes in Arabidopsis thaliana. The alternative donor splice site at the end of the first exon of PIN7 and PIN4, respectively, but not PIN3, results in two transcripts differing in 12 nucleotides. This sequence (orange) corresponds to the protein motif, located in the long internal hydrophilic loop of the transporter. There is also an additional PIN4c transcript present in publicly available transcriptomes.

(B) Amino acid alignment of the region around the 4-amino acid motif changed by AS in the PIN3 clade proteins (boxed in pink) in Arabidopsis thaliana, including the closest PIN paralogs.

(C) Table shows the number of RNA-seq reads spanning the exon1-exon2 junction corresponding to the detected PIN7 transcripts in selected Arabidopsis thaliana tissue sources. Their ratio was calculated as a percentage of total reads mapped to this area as assessed from the genome browser graphic interface.

(D) Protein sequence alignment showing the conservation of AS in the PIN3 clade of auxin transporters among rosids.

(E) Accumulation of [3H]NAA in BY-2 cells following induction of Arabidopsis thaliana G10-90::XVE>>AtPIN7a-GFP and G10-90::XVE>>AtPIN7b-GFP cDNAs with 1 µM β-estradiol. [3H]NAA accumulations within the observed period show no difference between both tested isoforms. The values shown in box plots were normalized to the average maximum of the [3H]NAA accumulation rates in the non-induced lines. Middle line shows median, the box corresponds to the 25% and 75% quartiles, the whiskers represent minima and maxima (n = 9).

See also Supplemental Figure 1.

PIN4- and *PIN7a* and *b* transcripts are expressed abundantly in all tissues, independently on the data set inspected. Besides these AS events, we also identified a minor *PIN4c* (Marquez et al., 2012; Hrtyan et al., 2015) splice isoform (but not corresponding *PIN7c*), which comprised around 3-7% of the *PIN4* exon1-exon2 spanning reads (Figures 1A and Supplemental Figure 1A). Other occasionally observed transcripts (also corresponding to the other exon junctions) were not repetitively seen among different RNA-seq data sets. It thereby appears that *PIN7* and *PIN4* are processed into two and three transcripts, respectively, and that *PIN7a* and *b* (or *PIN4a* and *b*) are expressed in most of the plant organs at comparable or nearly similar levels.

Functionally relevant AS events are commonly evolutionarily conserved (Keren et al., 2010; Reddy et al., 2013), therefore we sought for available validated transcripts to determine whether similar splicing events occur in orthologous *PIN3* clade genes in other dicot species (Bennett et al., 2014; O'Leary et al., 2016). We found examples of such mRNAs besides members of the *Brassicaceae* family, for instance, also in *Abrus precatorius* (*Fabaceae*), which documents the conservation of this AS event in rosids, a plant clade which diversified more than 100 million years ago (Li et al., 2019) (Figure 1D). *PIN4c* did not show any deeper evolutional conservation. Thus, at least some genes of the *PIN3* clade are regulated by the same type of AS, across several plant families, which suggests that these AS events may have a relevant biological function.

PIN7a and PIN7b transport auxin with comparable rates in tobacco cells

To test whether both protein isoforms indeed function as auxin transporters, we exemplified this on the expression of the *PIN7a* and *b* cDNA variants tagged with GFP, respecting the design of the original *PIN7-GFP* construct (Blilou et al., 2005), under the control of the β-estradiol-driven promoter in tobacco BY-2 cells (Petrasek et al., 2006; Müller et al., 2019). Following induction of both transgenes, we observed a comparable decrease of radioactive-labeled auxin accumulation inside the BY-2 cells (Figure 1E) and the time course of the auxin accumulation drop appeared to be similar for both constructs (Supplemental Figure 1B), in accord to that of *PIN7a* cDNA, examined previously (Petrasek et al., 2006). These experiments reveal that *PIN7a* and *PIN7b* code for true auxin exporters, which transport auxin at similar rates in tobacco cell cultures.

AS changes subcellular dynamics of PIN proteins

Polarity and dynamic intracellular trafficking are essential functional attributes of PINs (Adamowski and Friml, 2015). We expressed fluorescently-tagged cDNA versions of

the respective *PIN7* and *PIN4* transcripts under their native promoters in *Arabidopsis thaliana*. Their overall expression patterns resembled those of the *PIN7-GFP* and *PIN4-GFP* lines made on the basis of the genomic sequence (Supplemental Figures 2A-2D). At the cellular level, the protein isoform localization did not largely differ from each other in terms of polarity or general subcellular localization in the root tip (Figure 2A). Thus, at a given resolution, it appears that the motif substituted during AS does not change the basic subcellular localization or expression pattern of both PIN7 and PIN4 proteins.

The anterograde trafficking of proteins towards PM can be effectively blocked by the fungal toxin brefeldin A (BFA). It leads to internal accumulation of the membrane-bound PINs into characteristic BFA bodies (Geldner et al., 2001; Kleine-Vehn et al., 2010). During time-lapse imaging, we observed that while PIN7a-GFP accumulated readily in these intracellular aggregates, PIN7b-RFP formed less pronounced aggregates, co-localizing with PIN7a-GFP incompletely (Figures 2A and 2B; Supplemental Figure 2E). To exclude that the fluorescent tag influences the sensitivity of the PIN7 intracellular trafficking caused by BFA, we compared the response of PIN7a-GFP with additionally generated PIN7b-GFP cDNA expressing lines. We observed that the BFA mediated aggregation of PIN7b-GFP indeed showed a moderate delay, compared with PIN7a-GFP (Figure 2C). These observations suggest that the PIN7 isoforms differ in the speed of their intracellular trafficking pathways or delivery to the PM and the choice of the tag does not appear to interfere significantly with the subcellular dynamics of PIN7.

PIN polarity does not seem to strictly require the cytoskeleton (Glanc et al., 2018), but subcellular PIN trafficking has been proposed to be mediated by two distinct pathways (Geldner et al., 2001; Glanc et al., 2018). The first is dependent on actin filaments (cytochalasin D-sensitive) and occurs in most cells of the root meristem. The second (oryzalin-sensitive) utilizes microtubules and is linked with cytokinesis. Drugs that depolymerize actin filaments (cytochalasin D) and tubulin (oryzalin) (Geldner et al., 2001; Kleine-Vehn et al., 2008b) showed only little effect on the intracellular localization of both PIN7 isoforms when applied alone (Supplemental Figures 2F and S2G). Pretreatment with cytochalasin D prevented the formation of the BFA bodies (Geldner et al., 2001) containing both PIN7 isoforms (Figure 2D). Yet, when we applied oryzalin prior to the BFA treatment, the BFA compartments containing PIN7a-GFP and PIN7b-RFP associated in only very weakly co-localizing structures (Figure 2E).

Next, we tested how the cytoskeleton is involved in the trafficking of both PIN7 isoforms from the BFA bodies to the PM by washing out BFA with cytochalasin D or

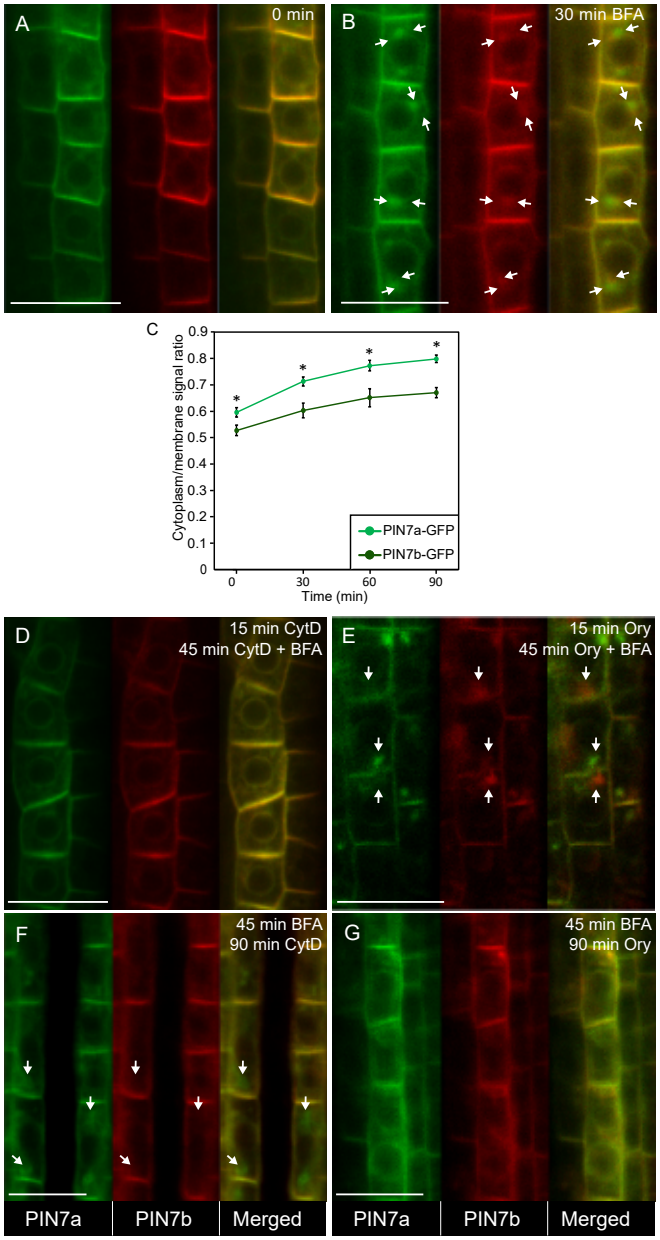

Figure 2. PIN7a-GFP and PIN7b-RFP cDNA-encoded proteins show similar cellular localization patterns but differ in response to brefeldin A (BFA) and the cytoskeletal drugs in the Arabidopsis primary root meristem.

(A) Subcellular localization and polarity of untreated PIN7a-GFP and PIN7b-RFP cDNA-encoded proteins in the primary root meristem cells.

(B) Both PIN7a-GFP and PIN7b-RFP aggregate in the intracellular compartments (BFA bodies) after 30 min of 50 µM BFA treatment, but do not fully co-localize (arrows).

(C) Temporal dynamics of BFA mediated aggregation of PIN7a-GFP and PIN7b-GFP inside cells. The values were determined as a ratio of fluorescence intensities between the cytoplasm and plasma membrane. (*$P < 0.05$ by ANOVA, $n = 12$). Data are means ± S. E.

(D) The fluorescence signal from PIN7a-GFP and PIN7b-RFP upon disruption of actin filaments with 20 µM cytochalasin D for 15 min followed by the addition of 50 µM BFA for another 45 min.

(E) PIN7a-GFP and PIN7b-RFP aggregation (arrows) upon disruption of microtubules with 20 µM oryzalin for 15 min, followed by the addition of 50 µM BFA for another 45 min.

(F) Effect of cytochalasin D on the PIN7a-GFP and PIN7b-RFP exit from the BFA bodies upon 45 min pre-treatment with 50 µM BFA and followed by wash-out with 20 µM cytochalasin D for another 90 min.

(G) Effect of oryzalin on the PIN7a-GFP and PIN7b-RFP exit from the BFA bodies upon 45 min pre-treatment with 50 µM BFA and followed by wash-out 20 µM oryzalin.

In (A, B and D-G), the signals of 3 cells in each of 5 root tips were analyzed ($n = 15$); bars, 10 µm.

See also Supplemental Figure 2.

oryzalin (Geldner et al., 2001). In the presence of cytochalasin D, PIN7a-GFP largely persisted inside the BFA bodies, while the PIN7b-RFP signal was almost absent in these aggregates (Figure 2F). We generally did not see any difference between both isoforms when BFA was washed out with oryzalin (Figure 2G). These data thereby suggest that both PIN7 isoforms use vesicle trafficking pathways that are assisted by a common cytoskeletal scaffold. These pathways differ in their dynamics and the endomembrane components involved and are consistent with previous findings that individual PINs can utilize multiple PM delivery routes (Boutté et al., 2006; Kleine-Vehn et al., 2008b).

AS affects dynamics of PIN7 at the PM but not its ability to relocate in response to tropic stimuli

Complementary to the observations obtained by the pharmacological approach, we tracked intracellular PIN7 dynamics under natural conditions. Auxin transporters of the PIN3 clade change their polar localization on the PM by the reaction to various environmental cues, in particular by switching the light or gravity vectors (Friml et al., 2002; Rakusová et al., 2011; Ding et al., 2011). PIN3 relocation in response to gravity in columella root cells is seen in as little as 2 min, while the relocation of PIN7-GFP requires approximately 30 min to be detected (Friml et al., 2002; Kleine-Vehn et al., 2010; Pernisova et al., 2016; Grones et al., 2018). We examined plants harboring both *PIN7a-GFP* and *PIN7b-RFP* cDNAs under short and long gravitropic stimuli. We did not find any difference in relocation dynamics between both isoforms in these experiments (Supplemental Figures 3A-3D). We observed no difference in the polarity change between PIN7a-GFP and PIN7b-RFP in hypocotyl gravitropic (Rakusová et al., 2011; Rakusová et al., 2016) and phototropic (Ding et al., 2011) bending assays (Supplemental Figures 3E-3I; due to limited transparency of hypocotyls, we used lines expressing the cDNAs under strong endodermal *SCARECROW* (*SCR*) promoter (Rakusová et al., 2011)). These data indicate that the different subcellular pathways driving both PIN7a-GFP and PIN7b-RFP cargos are not connected with their ability to change polarity in response to tropic stimuli.

Several studies employed the fluorescence recovery after photobleaching (FRAP) analysis to investigate the dynamic turnover of various proteins, including PINs, on PM (Men et al., 2008; Martinière et al., 2012; Langowski et al., 2016). We therefore bleached a region of the PM signal in the root meristem of the *PIN7a-GFP* and *PIN7b-GFP* cDNA lines and measured the FRAP in this area. Notably, PIN7a-GFP showed a slower recovery of fluorescence than PIN7b-GFP (Figure 3A). The difference in the recovery speed and also in

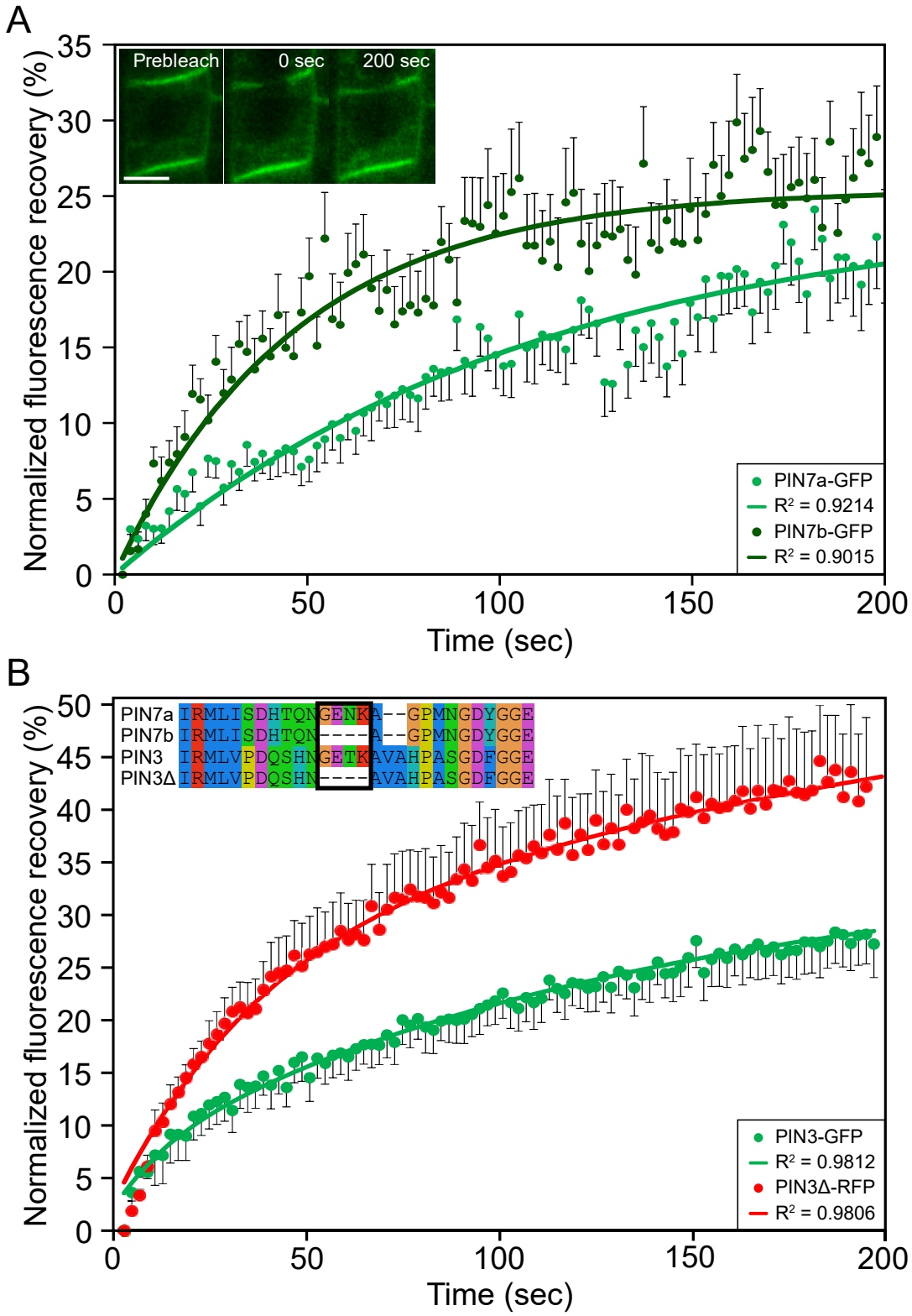

Figure 3. The cDNA encoded PIN7a and PIN7b isoforms tagged with fluorescent proteins show differential dynamics on the plasma membrane, as revealed by fluorescence recovery after photobleaching (FRAP).

(A) The PIN7a-GFP and PIN7b-GFP normalized FRAP, with single-phase exponential fitting curves. PIN7b-GFP shows different fluorescence recovery on the plasma membrane, compared to the longer PIN7a-GFP. The example image of the bleached region in cells is shown on the inset.

(B) The PIN3Δ-RFP and PIN3-GFP normalized FRAP, with single-phase exponential fitting curves. PIN3Δ-RFP, which lacks the 4 amino acid motif to mimic the properties of the PIN7b isoform, shows faster fluorescence recovery, in comparison to the control PIN3-GFP.
Bars, 5 µm. Data are means, error bars are ± S. E. At least 3 membranes in 5-6 root tips were analyzed in each experiment ($n \geq 20$).

See also Supplemental Figures 3 and 4.

the overall mobile phase ratio was even more pronounced when we used lines expressing both cDNAs under the stronger *SCR* promoter (Supplemental Figure 4A); the choice of GFP or RFP tag did not markedly interfere with the fluorescence recovery (Supplemental Figure 4B). To validate our observations further, we generated plants carrying a *PIN3::PIN3Δ-RFP* cDNA construct, which lacks the GETK motif corresponding to the four amino acids absent in PIN7b (Figures 1B and 3B). The PIN3Δ-RFP signal showed an incomplete co-localization with the wild type PIN3-GFP variant in the BFA bodies (Supplemental Figures 4C and 4D), and faster recovery on the PM, analogous to that observed for PIN7a and PIN7b (Figure 3B). It therefore appears that the motif altered by AS of PIN7 is required for the regulation of dynamics of individual isoforms within the PM.

***PIN7* splice isoforms are functionally different, based on the phenotype rescue tests**

To explore the role of the *PIN7* splice isoforms in plant development, we tested the ability of their fluorescently tagged cDNAs to complement the phenotypes associated with the *PIN7* locus. We initially selected the phototropic hypocotyl bending assay, which is highly dependent on the activity of the PIN3 clade proteins (Friml et al., 2002; Willige et al., 2013). We were unable to detect significant defects in the single *pin7-2* knockout (Friml et al., 2003) itself, even at a detailed temporal resolution (Supplemental Figure 5A). As weak phenotypes of the *pin7-2* loss of function mutants are the result of redundancy with other genes from the *PIN3* clade (Friml et al., 2003; Blilou et al., 2005; Willige et al., 2013), we further employed a triple *pin3-3 pin4-101 pin7-102* knock out (*pin347*) as a genetic background, which lacks the phototropic response almost completely (Willige et al., 2013). Here, *PIN7a-GFP* cDNA was able to rescue the phototropic bending, while the *PIN7b-RFP* cDNA did not show any effect, regardless of whether the native (Figure 4A) or a strong endodermal *SCR* promoter (Supplemental Figure 5B), was used. The choice of the tag does not appear to have any effect in these assays, as evidenced by the lines where the fluorophore sequences have been swapped (Figure 4B). Together, these data indicate that the motif changed by AS alters the function of the PIN7 protein in *Arabidopsis*.

PIN7a, but not *PIN7b*, cDNA rescues the *pin347* phenotypes in the hypocotyl bending test, and PIN3 clade auxin efflux carries have been implicated in numerous instances of auxin-mediated development. We therefore tested whether in some them the role of the particular isoform could be prevalent. These processes include: determining of root protoxylem formation (Bishopp et al., 2011) (Figure 4C), lateral root density (Swarup et al., 2008) (Figure 4D), vertical direction of the root growth (Friml et al., 2002; Kleine-Vehn et al.,

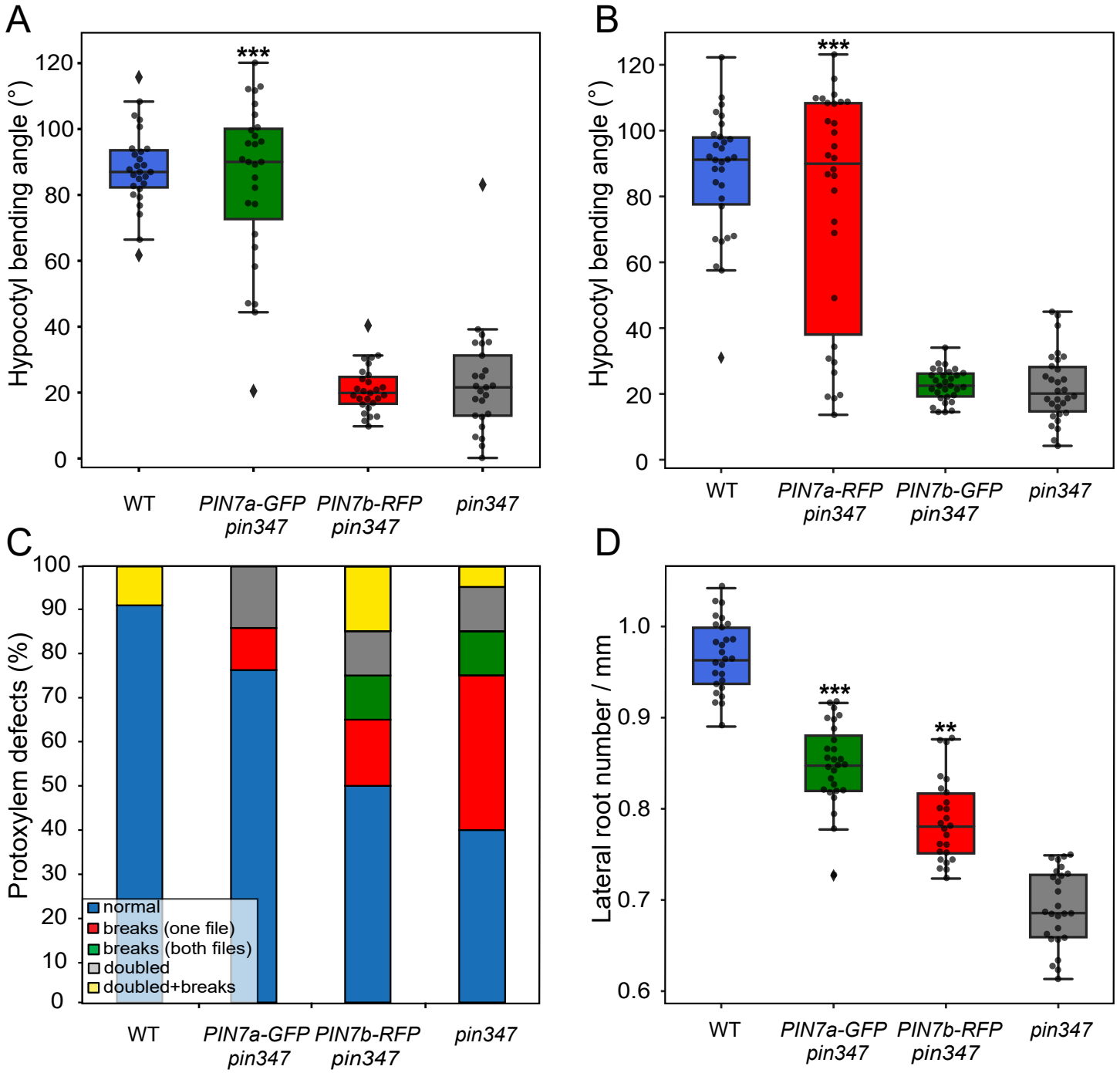

Figure 4. In contrast to PIN7b, the PIN7a cDNA under control of the natural PIN7 promoter complements phenotypes associated with the PIN7 locus.

(A) Phototropic bending of the etiolated pin347 seedlings carrying the PIN7a-GFP and PIN7b-RFP constructs.

(B) Phototropic bending of the etiolated pin347 seedlings carrying the PIN7a-RFP and PIN7b-GFP constructs.

(C and D) Quantification of the primary root protoxylem defects (C) and lateral root primordia (D) initiation of the pin347 seedlings harboring the PIN7a-RFP and PIN7b-GFP constructs.

On (A), (B) and (D), the middle line corresponds to median, the box corresponds to the 25% and 75% quartiles, the whiskers correspond to minima and maxima, dots represent single data points. The asterisks indicate significance between respective line and the pin347 mutant control (**$P < 0.01$, ***$P < 0.001$ by ANOVA). For each line in each experiment, at least 15 seedlings were analyzed ($n \geq 15$).

See also Supplemental Figure 5.

2010; Pernisova et al., 2016) (Supplemental Figure 5C), lateral root orthogravitropism (Rosquete et al., 2013) (Supplemental Figure 5D), gravity-induced hypocotyl bending (Rakusová et al., 2011) (Supplemental Figure 5E), number of rosette branches after decapitation (Bennett et al., 2016) (Supplemental Figure 5F) and the overall rosette size (Bennett et al., 2016) (Supplemental Figure 5G). Similar to the results above, the *PIN7a-GFP* cDNA usually almost completely rescued the tested phenotypes, while the contribution of *PIN7b-RFP* was smaller or even undetectable. This suggests that the functional roles of both isoforms are common, regardless of the phenotype observed.

A fluorescent reporter for studying the *PIN7a* and *b* expression

The levels of *PIN7* (and *PIN4*) AS transcripts seem to be at comparable levels in most organs (Figure 1C and Supplemental Figure 1A). However, this may not describe the actual situation at the resolution of individual cells. To address this, we designed a dual fluorescent reporter, which allows for monitoring the activity of the AS of *PIN7 in planta* and *in situ* (Figure 5A). Indeed, in the primary root or in the hypocotyl, we observed generally overlapping expression of both isoforms without any obvious tissue preference (Figure 5B; Supplemental Figure 6A). However, there were several instances in the vegetative tissue, where the ratio of reporter signals appears to be uneven. These include early lateral root primordia (Figure 5C), the mature pericycle adjacent to the phloem area (Supplemental Figure 6B), the stomatal lineage ground cells of the cotyledons (Supplemental Figure 6C), and the concave side of opening apical hook (Figures 5D), where the PIN7b-RFP signal prevailed over that of PIN7a-GFP. In general, these data corroborate the presence of both isoforms in most cells and suggest that they may function in a coordinated manner.

The combined activity of both PIN7a and PIN7b is required for apical hook formation and tropic responses

The occasional exaggerated response of the *pin347* mutants containing the *PIN7a-GFP* transgene (Supplemental Figure 5E) prompted us to re-design phenotypic tests and adapt our experimental methodology to carefully record the temporal dynamics of the processes linked with the PIN3 clade function. We turned to apical hook development where the time scale measurements of the PIN-mediated development have been well established (Zadnikova et al., 2010). We also analyzed *pin4-101 pin7-102* (*pin34*) mutants and a newly generated *pin347* line that carried a combination of both *PIN7* cDNA constructs. Similar to gravi- and phototropic experiments, the *PIN7b-RFP* cDNA generally did not complement the severe

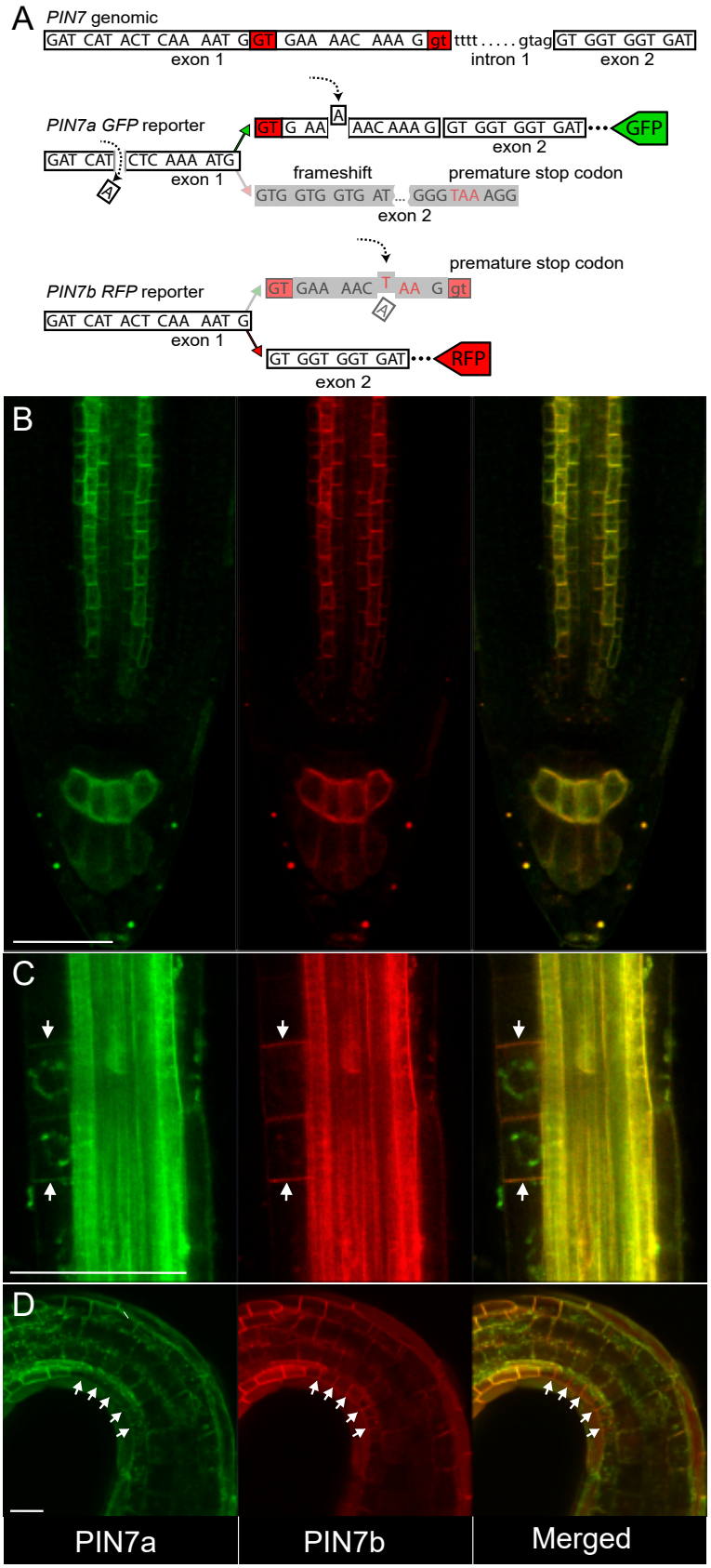

Figure 5. Reporter-based expression analysis of PIN7a and PIN7b isoforms across tissues.

(A) A scheme of the PIN7 splicing reporter. The reporter consists of two constructs: the PIN7a-GFP part contains two point mutations (marked with dashed arrows) and leads to the frameshift and its subsequent restoration when the PIN7a transcript is solely produced. PIN7b-RFP reporter carries a premature stop codon inside the protruding PIN7a region (dashed arrow below).

(B) PIN7a-GFP and PIN7b-RFP expression overlap in the root tip.

(C and D) PIN7b-RFP expression (arrows) PIN7a-GFP in the early lateral root primordia (C) and in the epidermis on the concave side of apical hook (D). The green signal in the perinuclear region of the lateral root primordia is an autofluorescence artifact.
For each tissue, at least 10 plants were analyzed ($n \geq 10$). Bars, 50 µm.

See also Supplemental Figure 6.

pin347 phenotype. Expression of the *PIN7a-GFP* cDNA in *pin347* indeed led to partial rescue of the apical hook formation defects, even surpassing the values observed for *pin34*. Surprisingly, the simultaneous expression of both *PIN7a-GFP* and *PIN7b-RFP* suppressed the dominant effects conferred by the *PIN7a-GFP* cDNA alone and phenocopied the *pin34* mutant (Figure 6A; this effect was not caused by suppressing the expression of PIN7a-GFP by the other transgene, Supplemental Figure 6D). This strongly suggests that both isoforms act in a mutually opposing manner to modulate the processes of apical hook development.

Apical hook formation is a complex process that involves several bending steps (Zadnikova et al., 2010), and the splicing reporter suggests a slightly different expression pattern of *PIN7a* and *b* isoforms during apical hook development (Figure 5D). The hypocotyl phototropic and gravity response includes only a single bending (Rakusová et al., 2011; Rakusová et al., 2016), and the expression of the reporter appears to be uniform in the respective tissue (Supplemental Figure 6A). Tracking dynamic bending of hypocotyls can thus provide a hint to whether one can account for the antagonistic behavior of both isoforms to differential expression or to their different dynamics during subcellular trafficking or at the PM. Similar to apical hook development (Figure 6A), introducing the *PIN7b-RFP* cDNA did not have any effect on the *pin347* phenotype, while the expression of *PIN7a-GFP* lead to more rapid bending than that observed for the *pin34* mutant. Finally, the presence of both *PIN7a-GFP* and *PIN7b-RFP* cDNAs in *pin347* was reminiscent of the *pin34* phenotype in both phototropic and gravity assays (Figures 6B and 6C). We therefore conclude that the shared activity of both PIN7 isoforms, likely conferred by their different trafficking or PM retention properties, but probably not by their differential expression, is required for proper apical hook formation and auxin-mediated tropic responses.

DISCUSSION

In this study, we show that AS diversifies the portfolio of PIN proteins present in *Arabidopsis thaliana*. At the cellular level, AS does not alter the ability of the PIN7 proteins to transport auxin *per se* or their overall subcellular localization, but it changes their dynamics on the PM. In general, AS modifies protein properties variably. It can affect protein subcellular localization, ligand binding affinity, enzymatic or transporting activities, protein stability or the presence of covalent post-translational modifications (Stamm et al., 2005; Kelemen et al., 2013). Different covalent modifications alter the subcellular trafficking of most PINs. Phosphorylation sites on serine, threonine or tyrosine residues of various PINs have been identified; their phosphorylation status also changes PIN-mediated tropic responses

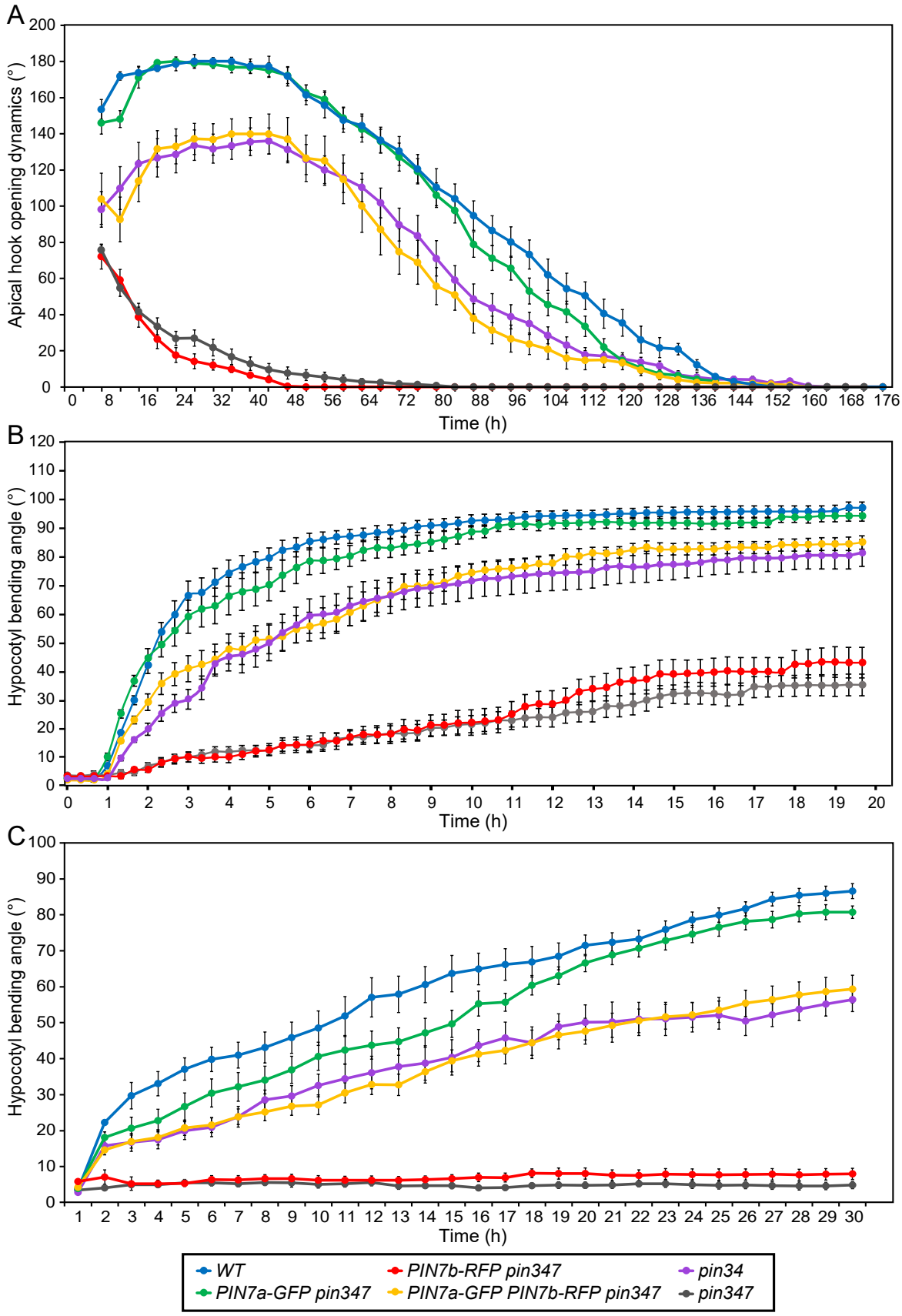

Figure 6. The simultaneous presence of PIN7a-GFP and PIN7b-RFP cDNA constructs in pin347 phenocopies the pin34 knock out mutant during apical hook opening and hypocotyl gravitropic bending.

(A-C) Temporal dynamics of etiolated pin347 seedlings carrying the PIN7a-GFP and PIN7b-RFP transgenes examined (A) during apical hook development, (B) hypocotyl phototropic and (C) gravitropic bending.
Data are means ± S. E. For each data point, the values obtained from 15 vertically grown seedlings were assessed (n = 15).

(Rademacher and Offringa, 2012; Barbosa et al., 2018; Zwiewka et al., 2019). Also PIN ubiquitination (on lysines) and controlled proteolytic degradation act in auxin-mediated processes (Leitner et al., 2012). However, none of the candidate residues required for these modifications is present in the vicinity of the amino acid motif changed by AS. This region, present inside the PIN long hydrophilic loop shows low amino acid conservation and it is perhaps intrinsically disordered (Figure 1C) (Zwiewka et al., 2019). One can therefore speculate whether it may change, perhaps by its length, the ability to assemble internal PIN domains within the long hydrophilic group (Buljan et al., 2013) and modulate their interaction affinity with other factors required for the entry and presence in secretory pathways and/or for PIN7 dynamics at the PM.

We also present genetic evidence that the mutual activity of PIN7a and PIN7b is operational during apical hook formation and tropic responses. We also tested major functional aspects linked with the cellular activity of PIN7 that might be responsible for the observed phenotypes (Adamowski and Friml, 2015). We found the differences between PIN7a and PIN7b at the level of the PM recycling pathways and the stability on the plasma membrane. It was previously demonstrated that the dynamics of PINs on the PM is controlled in principle by two factors: by lateral diffusion in earlier phases and by dynamic recycling from the secretory pathways in longer timelines (Kleine-Vehn et al., 2008a; Kleine-Vehn et al., 2011; Langowski et al., 2016). As the effect of secretion or recycling has been evidenced to be minor within 10 min after photobleaching (Kleine-Vehn et al., 2011; Langowski et al., 2016), it seems that lateral diffusion significantly participates on the differential behavior of PIN7a and PIN7b. In accordance with previous findings (Kleine-Vehn et al., 2011; Feraru et al., 2011; Langowski et al., 2016), slower PIN7a FRAP rates suggest that PIN7 properly functions when only associated with a larger complex or inside stable membrane clusters. According to the earlier published model (Langowski et al., 2016), it therefore seems that PIN7b probably antagonizes PIN7a action by impeding the polar auxin flow provided by PIN7a in these membrane domains (Supplemental Figure 6E).

The mutually antagonistic interaction between two splice isoforms (or a similar coordinated mechanism) has generally been already proposed in *Arabidopsis* (Szakonyi and Duque, 2018). The seed dormancy regulator *DELAY OF GERMINATION 1* (*DOG1*) is processed into five mRNAs. Only the expression of two or more DOG1 cDNAs under the native promoter rescues the *dog1* phenotype by synergistic stabilization of the protein by its multimerization (Nakabayashi et al., 2015). The transcriptional factor HYH (HY5 HOMOLOG) possesses an isoform, which lacks a domain required for proteasomal

degradation, which leads to its increased stability and probably works as a semi-dominant splice variant (Sibout et al., 2006; Szakonyi and Duque, 2018). The example of AS of PIN7 is thus one of the first instances in plants where the mutually antagonistic effects of two splice isoforms are observed on a single gene.

EXPERIMENTAL PROCEDURES

Plant material and plant growth conditions

All plant material, except tobacco cell cultures, was in the *Arabidopsis thaliana* (L.) Heynh., Col-0 ecotype. These mutant and transgenic lines were described previously: *PIN3::PIN3-GFP* (Zadnikova et al., 2010), *PIN4::PIN4-GFP*, *PIN7::PIN7-GFP* (Blilou et al., 2005), *pin3-3 pin4-101 pin7-102* (*pin347*), *pin3-3 pin4-101* (*pin34*) (Willige et al., 2013), *pin7-2* (Friml et al., 2003).

For the *in vitro* cultivation, the seeds were surface-sterilized for 5 h with chlorine gas, plated on 0.5× Murashige & Skoog medium with 1 % sucrose, and then stratified for 2 d at 4°C in darkness. Unless indicated otherwise, the seedlings were grown on vertically oriented plates for 4-6 days under 16 h : 8 h photoperiod, 22 : 18°C, light : dark.

The following chemicals were used for treatments: brefeldin A (BFA), cytochalasin D (CytD), oryzalin (Ory), β-estradiol, 2,4-dichlorophenoxyacetic acid (2,4-D), all from Sigma (Sigma-Aldrich, St. Louis, MO, USA). Radioactively labeled auxin accumulation assays were performed with [^{3}H]NAA (naphthalene-1-acetic acid; 20 Ci.mmol^{-1}; American Radiolabeled Chemicals, St. Louis, MO, USA).

DNA manipulations and transgenic work

The genomic *PIN7::PIN7-RFP* construct was made by replacing the GFP coding sequence in the original *PIN7::PIN7-GFP* construct (Blilou et al., 2005). For creating the *PIN7(4)*::*PIN7(4)a-GFP* and *PIN7(4)*::*PIN7(4)b-RFP* cDNA constructs, the respective cDNAs were cloned into the pDONR221 P5-P2 entry vector (Invitrogen, Life Technologies, Carlsbad, CA., USA) by the Gateway BP reaction (Invitrogen). The *Xba*I restriction site was introduced at the 1350 bp (for *PIN7*) or 1341 bp (for *PIN4*) position of the cDNA coding region for placing the fluorophore tag sequence. In parallel, the *PIN7* (or *PIN4*) promoters were inserted into the pH7WG Gateway vector (Department of Plant Systems Biology, Ghent University, Belgium; Karimi et al., 2002) by the Gibson Assembly kit (New England Biolabs, Ipswich, MA, USA). The tagged *PIN7* and *PIN4* cDNA entry clones were then recombined with the modified pH7WG destination vector by the Gateway LR reaction (Invitrogen). For

the cloning of the *PIN7* splicing dual fluorescent reporter, the entry vectors carrying the genomic sequence of *PIN7-GFP* and *PIN7-RFP* (Adamowski and Friml, 2015), respectively, were modified by inverse PCR. The resulting constructs were then recombined by the Gateway LR reaction with the *PIN7* promoter containing the pH7WG destination vector. The *SCR::PIN7a-GFP* and *SCR::PIN7b-RFP* constructs were obtained by recombination of the *SCR* promoter in pDONR221 P1-P5r and *PIN7* cDNA entry clones with the pH7WG destination vector by the Multisite Gateway LR reaction. *PIN3Δ-RFP* cDNA was custom synthesized (Gen9, Ginkgo Bioworks, Boston, MA, USA), cloned into pDONR221 P5-P2 vector and together with the *PIN3* promoter pDONR221 P1-P5r construct recombined into the pH7WG vector with Multisite Gateway. The validated binary constructs were transformed into *Arabidopsis* by floral dipping. For making the estradiol-inducible *G10-90::XVE>>AtPIN7(4)a-GFP*, and *G10-90::XVE>>AtPIN7(4)b-GFP* constructs, tagged *PIN7* or *PIN4* cDNA entry clones were recombined with the pMDC7 destination vector (Curtis and Grossniklaus, 2003) by the Gateway LR reaction. Unless stated otherwise, the constructs present in the study were cloned under their natural *PIN4* or *PIN7* promoter. Primers used in this work are listed in Supplemental Table 1.

For the generation of the stable transgenic lines carrying the cDNA constructs, at least eight independent descendant populations of primary transformants were preselected for the presence of the fluorescent signal. The functional validity of the cDNA constructs was verified in the phototropic bending test, where all candidate lines matched the presented results. Selected lines were used for further phenotypic analysis.

Plant phenotype analysis

The dynamic seedling development was tracked in the custom made dynamic morphogenesis observation chamber equipped with blue and white LED unilateral light sources, infra-red LED back light and a camera for imaging in the infra-red spectra, controlled by the Raspberry Pi3B microcomputer (Raspberry Pi foundation, Cambridge, UK). For the hypocotyl bending assays, the plated seeds were first illuminated for 6 h with white light. The plates were then transferred to the observation chamber for 3-4 d. For the hypocotyl phototropic bending experiments (Friml et al., 2002), the dark-grown seedlings were afterward illuminated for 20 h with unilateral white light and imaged every 20 minutes. For hypocotyl gravitropic bending experiments (Rakusová et al., 2011), the dark-grown seedlings were rotated by 90° clockwise and imaged for 30 h every 60 min. For tracking apical hook development, the seeds were first illuminated for 6 h with white light. They were then

transferred to the observation chamber and their development recorded every 4 h for a total 150 - 200 h in infrared spectra. Germination time was set as time 0, when first traces of the main root were observed, individually for each seedling analyzed. Apical hook was determined as an angle between the immobile (non-bending) part of hypocotyl and the distal edge of cotyledons (Zadnikova et al., 2010), using the ImageJ software (Rueden et al., 2017). At least 15 seedlings were analyzed for each line. Each experiment was done at least three times.

For protoxylem defects analysis, 5-d old light-grown seedlings were cleared and analyzed as described previously (Bishopp et al., 2011). For examining lateral root density, 8-d old light-grown seedlings were cleared and observed with a DIC microscope (Dubrovsky et al., 2009). Lateral root density was calculated by dividing the total number of lateral roots and lateral root primordia to the length of the main root as described (Dubrovsky et al., 2009). Vertical Growth Index (VGI), defined as a ratio between main root ordinate and main root length, was quantified on 5-d old seedlings as published previously (Grabov et al., 2005). For measuring the Gravitropic Set-point Angle (GSA), plates with 14-d old light-grown seedlings were scanned and the angles between the vertical axis and five innermost 0.5 mm parts of lateral root were determined as described previously (Roychoudhry et al., 2017). In all cases, 12-20 seedlings were analyzed for each line. Each experiment was done at least three times.

For decapitation experiments, 4-week short-day grown plants were moved into long-day conditions to induce flowering. After the primary bolt reached 10-15 cm, the plant was decapitated. The number of rosette branches was recorded at 7, 10 and 14-d after decapitation (Greb et al., 2003; Waldie and Leyser, 2018). Rosette size was inspected in 18-d light-grown plants prior to documenting. 10 plants were analyzed for each line, the experiment was done three times.

Microscopy

Bright-field microscopy (differential interference contrast, DIC) was conducted on the Olympus BX61 instrument (Olympus, Shinjuku, Tokyo, Japan) equipped with a DP50 camera (Olympus). Routine confocal microscopy was performed on inverted Zeiss Axio Observer.Z1 containing the standard confocal LSM880 and Airyscan modules with 20x/0.8 DIC M27 air, 40x/1.2 W Kor FCS M27 air and 63x/1.40 Oil DIC M27 objectives (Carl Zeiss AG, Jena, Germany). Gravity-induced polarity change experiments were carried out on Zeiss Axio Observer.Z1 with vertically oriented sample position and the 40x/0.75 glycerol objective.

To observe the light-induced polarity change of PIN7a-GFP and PIN7b-RFP, 4-d dark-grown seedlings were irradiated for 4 h with unilateral white light and then imaged with Zeiss Axio Observer.Z1 LSM880 with a vertically oriented sample position, as described (Willige et al., 2013). For analyzing gravity-induced polarity change, 4-d dark-grown seedlings were reoriented by 90° clockwise and imaged 6 and 24 h after rotation, as described (Rakusová et al., 2011).

For BFA treatments, 5-d light-grown seedlings were transferred to liquid 0.5× MS media containing 50 µM BFA. The membrane/cytosol ratio was determined with ImageJ, it was defined as the mean membrane signal intensity divided by the mean fluorescence in the cytosol. For cytoskeleton depolymerizing drug treatments (Geldner et al., 2001), 5-d light-grown seedlings were transferred to liquid 0.5× MS media supplemented with 20 µM of cytochalasin D or 20 µM oryzalin. The co-treatments were done by the direct addition of BFA. For the BFA removal, prior to the addition of the cytoskeleton depolymerizing compounds, seedlings were twice washed out with fresh media and then transferred to that supplemented with the respective cytoskeleton-depolymerizing drug.

Fluorescent recovery after photobleaching (FRAP)

For the FRAP experiments, Zeiss Axio Observer.Z1 equipped with the LSM880 confocal and Airyscan modules and the 40x/1.2 W Kor FCS M27 air objective was used. A rectangular region of interest (ROI) of 40 x 20 pixels was selected on the basal or apical PM of cells inside the vascular cylinder in the primary root meristematic area of 5-d light-growth seedlings. ROI was bleached with the maximum 488 nm laser intensity and fluorescence recovery was documented every 1 or 2 sec for a total 200 sec. Recovery time lapses were analyzed with ImageJ. The Slices Alignment plugin (Tseng et al., 2012) for ImageJ was used for the elimination of cell movement caused by root growth. In parallel, another rectangular ROI (100 x 20 pixels) on the non-bleached cell was selected as a reference. To compensate for the fluorophore bleaching during the recovery period, the data were normalized using equation (Laňková et al., 2016)

$$In = \frac{\left(\frac{It}{It_{ref}}\right) - \left(\frac{Imin}{Imin_{ref}}\right)}{\left(\frac{Imax}{Imax_{ref}}\right) - \left(\frac{Imin}{Imin_{ref}}\right)},$$

where *In* is normalized fluorescence intensity, *It* is the intensity at the specific time point, *Imax* is the intensity after the initial bleaching, *Imax* is the intensity before initial bleaching. It_{ref}, $Imax_{ref}$ and $Imin_{ref}$ represent the same values for the reference ROI. At least 3 membranes

in 4-5 root tips were analyzed in each experiment. Single-phase exponential fitting was applied to the normalized FRAP data (SigmaPlot, Systat Software, Chicago, ILL, US) as described (Sprague and McNally, 2005; Laňková et al., 2016). Recovery half-time is defined as a time required for the fluorescence recovery to reach half of the steady-state fluorescence intensity (Soumpasis, 1983; Sprague and McNally, 2005).

Tobacco cell lines and auxin accumulation assays

Tobacco cell line BY-2 (*Nicotiana tabacum* L. cv. Bright Yellow 2) was cultivated as described (Müller et al., 2019). BY-2 cells were transformed with the pMDC7 constructs by co-cultivation with *Agrobacterium tumefaciens* strain GV2260 as earlier described (Petrasek et al., 2006; Müller et al., 2019). The transgene expression was maintained by cultivation on media supplemented with 40 $\mu g.ml^{-1}$ hygromycin (Roche) and 100 $\mu g.ml^{-1}$ cefotaxime (Sigma). Accumulation assays of radioactively labeled auxin were performed as previously published (Delbarre et al., 1996; Petrasek et al., 2006) with cells cultured for 2 days in β-estradiol or DMSO mock treatments. Presented results are from 3 biological replicates for each representative *PIN7a* and *PIN7b* line and were confirmed for each on two other independent genotypes. Independent β-estradiol inductions were done within 3-9 months after the establishment of the cell suspension on lines, which showed comparable levels of the expressed PIN7-GFP signal.

Statistics and sequence analysis

For two groups mean comparison, Student's *t*-test was applied. Statistical analysis of multiple groups was performed by one-way ANOVA with subsequent Tukey HSD post-hoc test. All statistical tests, including normality tests, were performed in R-studio IDE (R-studio, Boston, MA, USA). In the box plots, the whisker length was defined as $Q \pm 1.5 \times \mathrm{IQR}$, where Q is the corresponding quartile and IQR is the interquartile range. For creating the multiple sequence alignments, the protein sequences were aligned using the Clustal Omega algorithm (Sievers et al., 2011) and graphically outlined by Mega-X, using default ClustalX color code (Kumar et al., 2018).

ACKNOWLEDGMENT

We thank Claus Schwechheimer for the *pin34* and *pin347* seeds, Huibin Han for assistance with the hypocotyl imaging, Dmitry Konovalov for help with the evolutional analysis, Karel Müller for the initial qRT-PCR analyses of the tobacco cell lines and Ksenia

Timofeyenko and Jozef Mravec for discussions. This work was supported by the Czech Science Foundation (16-26428S) to I. K., M. H. and K. R, and the Ministry of Education, Youth and Sports of the Czech Republic (MEYS, CZ.02.1.01/0.0/0.0/16_019/0000738) to K. R. Imaging Facility of the Institute of Experimental Botany is supported by MEYS (projects LM2018129 - Czech BioImaging, ERDF CZ.02.1.01/0.0/0.0/16_013/0001775 and OPPK CZ.2.16/3.1.00/21519).

AUTHOR CONTRIBUTIONS

I. K., M. H., R. F., Z. V., D. R., and J. P. conducted experiments. J. H. enabled making part of this project in his laboratory. S. S. and J. F. provided unpublished material. I. K., J. P., T. B. J., M. J. F., J. F., J. P., and K. R. conceived the research and designed experiments. K. R. and I. K. wrote the manuscript. All authors read and commented on the final version of the manuscript.

DECLARATION OF INTERESTS

The authors declare no competing interests.

REFERENCES

Adamowski, M., and Friml, J. (2015). PIN-Dependent Auxin Transport: Action, Regulation, and Evolution. *Plant Cell* **27**:20–32.

Barbosa, I. C. R., Hammes, U. Z., and Schwechheimer, C. (2018). Activation and Polarity Control of PIN-FORMED Auxin Transporters by Phosphorylation. *Trends in Plant Science* **23**:523–538.

Bazin, J., Romero, N., Rigo, R., Charon, C., Blein, T., Ariel, F., and Crespi, M. (2018). Nuclear Speckle RNA Binding Proteins Remodel Alternative Splicing and the Non-coding Arabidopsis Transcriptome to Regulate a Cross-Talk Between Auxin and Immune Responses. *Front Plant Sci* **9**:1209.

Bennett, T., Brockington, S. F., Rothfels, C., Graham, S. W., Stevenson, D., Kutchan, T., Rolf, M., Thomas, P., Wong, G. K.-S., Leyser, O., et al. (2014). Paralogous Radiations of PIN Proteins with Multiple Origins of Noncanonical PIN Structure. *Mol Biol Evol* **31**:2042–2060.

Bennett, T., Hines, G., Rongen, M. van, Waldie, T., Sawchuk, M. G., Scarpella, E., Ljung, K., and Leyser, O. (2016). Connective Auxin Transport in the Shoot Facilitates Communication between Shoot Apices. *PLOS Biology* **14**:e1002446.

Bishopp, A., Help, H., El-Showk, S., Weijers, D., Scheres, B., Friml, J., Benková, E., Mähönen, A. P., and Helariutta, Y. (2011). A mutually inhibitory interaction

between auxin and cytokinin specifies vascular pattern in roots. *Curr. Biol.* **21**:917–926.

Blencowe, B. J. (2017). The Relationship between Alternative Splicing and Proteomic Complexity. *Trends in Biochemical Sciences* **42**:407–408.

Blilou, I., Xu, J., Wildwater, M., Willemsen, V., Paponov, I., Friml, J., Heidstra, R., Aida, M., Palme, K., and Scheres, B. (2005). The PIN auxin efflux facilitator network controls growth and patterning in Arabidopsis roots. *Nature* **433**:39–44.

Boutté, Y., Crosnier, M.-T., Carraro, N., Traas, J., and Satiat-Jeunemaitre, B. (2006). The plasma membrane recycling pathway and cell polarity in plants: studies on PIN proteins. *J. Cell. Sci.* **119**:1255–1265.

Buljan, M., Chalancon, G., Dunker, A. K., Bateman, A., Balaji, S., Fuxreiter, M., and Babu, M. M. (2013). Alternative splicing of intrinsically disordered regions and rewiring of protein interactions. *Current Opinion in Structural Biology* **23**:443–450.

Casson, S. A., Topping, J. F., and Lindsey, K. (2009). MERISTEM-DEFECTIVE, an RS domain protein, is required for the correct meristem patterning and function in Arabidopsis. *The Plant Journal* **57**:857–869.

Cheng, C.-Y., Krishnakumar, V., Chan, A. P., Thibaud‐Nissen, F., Schobel, S., and Town, C. D. (2017). Araport11: a complete reannotation of the Arabidopsis thaliana reference genome. *The Plant Journal* **89**:789–804.

Curtis, M. D., and Grossniklaus, U. (2003). A gateway cloning vector set for high-throughput functional analysis of genes in planta. *Plant Physiol.* **133**:462–469.

Darracq, A., and Adams, K. L. (2013). Features of evolutionarily conserved alternative splicing events between Brassica and Arabidopsis. *New Phytologist* **199**:252–263.

Delbarre, A., Muller, P., Imhoff, V., and Guern, J. (1996). Comparison of mechanisms controlling uptake and accumulation of 2,4-dichlorophenoxy acetic acid, naphthalene-1-acetic acid, and indole-3-acetic acid in suspension-cultured tobacco cells. *Planta* **198**:532–541.

Ding, Z., Galván-Ampudia, C. S., Demarsy, E., Łangowski, Ł., Kleine-Vehn, J., Fan, Y., Morita, M. T., Tasaka, M., Fankhauser, C., Offringa, R., et al. (2011). Light-mediated polarization of the PIN3 auxin transporter for the phototropic response in Arabidopsis. *Nat Cell Biol* **13**:447–452.

Dubrovsky, J. G., Soukup, A., Napsucialy-Mendivil, S., Jeknic, Z., and Ivanchenko, M. G. (2009). The lateral root initiation index: an integrative measure of primordium formation. *Ann. Bot.* **103**:807–817.

Feraru, E., Feraru, M. I., Kleine-Vehn, J., Martinière, A., Mouille, G., Vanneste, S., Vernhettes, S., Runions, J., and Friml, J. (2011). PIN Polarity Maintenance by the Cell Wall in Arabidopsis. *Current Biology* **21**:338–343.

Friml, J., Wiśniewska, J., Benková, E., Mendgen, K., and Palme, K. (2002). Lateral relocation of auxin efflux regulator PIN3 mediates tropism in Arabidopsis. *Nature* **415**:806–809.

Friml, J., Vieten, A., Sauer, M., Weijers, D., Schwarz, H., Hamann, T., Offringa, R., and Jürgens, G. (2003). Efflux-dependent auxin gradients establish the apical-basal axis of Arabidopsis. *Nature* **426**:147–153.

Ganguly, A., Park, M., Kesawat, M. S., and Cho, H.-T. (2014). Functional Analysis of the Hydrophilic Loop in Intracellular Trafficking of Arabidopsis PIN-FORMED Proteins. *Plant Cell* **26**:1570–1585.

Geldner, N., Friml, J., Stierhof, Y. D., Jürgens, G., and Palme, K. (2001). Auxin transport inhibitors block PIN1 cycling and vesicle trafficking. *Nature* **413**:425–428.

Ghelli, R., Brunetti, P., Napoli, N., Paolis, A. D., Cecchetti, V., Tsuge, T., Serino, G., Matsui, M., Mele, G., Rinaldi, G., et al. (2018). A Newly Identified Flower-Specific Splice Variant of AUXIN RESPONSE FACTOR8 Regulates Stamen Elongation and Endothecium Lignification in Arabidopsis. *Plant Cell* **30**:620–637.

Glanc, M., Fendrych, M., and Friml, J. (2018). Mechanistic framework for cell-intrinsic re-establishment of PIN2 polarity after cell division. *Nat. Plants* **4**:1082–1088.

Grabov, A., Ashley, M. K., Rigas, S., Hatzopoulos, P., Dolan, L., and Vicente-Agullo, F. (2005). Morphometric analysis of root shape. *New Phytol.* **165**:641–651.

Greb, T., Clarenz, O., Schafer, E., Muller, D., Herrero, R., Schmitz, G., and Theres, K. (2003). Molecular analysis of the LATERAL SUPPRESSOR gene in Arabidopsis reveals a conserved control mechanism for axillary meristem formation. *Genes Dev.* **17**:1175–1187.

Grones, P., Abas, M., Hajný, J., Jones, A., Waidmann, S., Kleine-Vehn, J., and Friml, J. (2018). PID/WAG-mediated phosphorylation of the Arabidopsis PIN3 auxin transporter mediates polarity switches during gravitropism. *Sci Rep* **8**:10279.

Hrtyan, M., Šliková, E., Hejátko, J., and Růžička, K. (2015). RNA processing in auxin and cytokinin pathways. *J. Exp. Bot.* **66**:4897–4912.

Kalyna, M., Lopato, S., and Barta, A. (2003). Ectopic Expression of atRSZ33 Reveals Its Function in Splicing and Causes Pleiotropic Changes in Development. *Mol. Biol. Cell* **14**:3565–3577.

Karimi, M., Inzé, D., and Depicker, A. (2002). GATEWAY^{TM} vectors for Agrobacterium-mediated plant transformation. *Trends in Plant Science* **7**:193–195.

Kelemen, O., Convertini, P., Zhang, Z., Wen, Y., Shen, M., Falaleeva, M., and Stamm, S. (2013). Function of alternative splicing. *Gene* **514**:1–30.

Keren, H., Lev-Maor, G., and Ast, G. (2010). Alternative splicing and evolution: diversification, exon definition and function. *Nat Rev Genet* **11**:345–355.

Kleine-Vehn, J., Dhonukshe, P., Sauer, M., Brewer, P. B., Wiśniewska, J., Paciorek, T., Benková, E., and Friml, J. (2008a). ARF GEF-Dependent Transcytosis and Polar Delivery of PIN Auxin Carriers in Arabidopsis. *Current Biology* **18**:526–531.

Kleine-Vehn, J., Łangowski, Ł., Wiśniewska, J., Dhonukshe, P., Brewer, P. B., and Friml, J. (2008b). Cellular and Molecular Requirements for Polar PIN Targeting and Transcytosis in Plants. *Molecular Plant* **1**:1056–1066.

Kleine-Vehn, J., Ding, Z., Jones, A. R., Tasaka, M., Morita, M. T., and Friml, J. (2010). Gravity-induced PIN transcytosis for polarization of auxin fluxes in gravity-sensing root cells. *PNAS* **107**:22344–22349.

Kleine-Vehn, J., Wabnik, K., Martinière, A., Łangowski, Ł., Willig, K., Naramoto, S., Leitner, J., Tanaka, H., Jakobs, S., Robert, S., et al. (2011). Recycling, clustering, and endocytosis jointly maintain PIN auxin carrier polarity at the plasma membrane. *Molecular Systems Biology* **7**:540.

Klepikova, A. V., Kasianov, A. S., Gerasimov, E. S., Logacheva, M. D., and Penin, A. A. (2016). A high resolution map of the Arabidopsis thaliana developmental transcriptome based on RNA-seq profiling. *Plant J.* **88**:1058–1070.

Kriechbaumer, V., Wang, P., Hawes, C., and Abell, B. M. (2012). Alternative splicing of the auxin biosynthesis gene YUCCA4 determines its subcellular compartmentation. *Plant J.* **70**:292–302.

Kumar, S., Stecher, G., Li, M., Knyaz, C., and Tamura, K. (2018). MEGA X: Molecular Evolutionary Genetics Analysis across Computing Platforms. *Molecular Biology and Evolution* **35**:1547–1549.

Langowski, L., Wabnik, K., Li, H., Vanneste, S., Naramoto, S., Tanaka, H., and Friml, J. (2016). Cellular mechanisms for cargo delivery and polarity maintenance at different polar domains in plant cells. *Cell Discov* **2**:16018.

Laňková, M., Humpolíčková, J., Vosolsobě, S., Cit, Z., Lacek, J., Čovan, M., Čovanová, M., Hof, M., and Petrášek, J. (2016). Determination of Dynamics of Plant Plasma Membrane Proteins with Fluorescence Recovery and Raster Image Correlation Spectroscopy. *Microscopy and Microanalysis* **22**:290–299.

Leitner, J., Petrášek, J., Tomanov, K., Retzer, K., Pařezová, M., Korbei, B., Bachmair, A., Zažímalová, E., and Luschnig, C. (2012). Lysine63-linked ubiquitylation of PIN2 auxin carrier protein governs hormonally controlled adaptation of Arabidopsis root growth. *PNAS* **109**:8322–8327.

Li, H.-T., Yi, T.-S., Gao, L.-M., Ma, P.-F., Zhang, T., Yang, J.-B., Gitzendanner, M. A., Fritsch, P. W., Cai, J., Luo, Y., et al. (2019). Origin of angiosperms and the puzzle of the Jurassic gap. *Nat. Plants* **5**:461–470.

Marquez, Y., Brown, J. W. S., Simpson, C., Barta, A., and Kalyna, M. (2012). Transcriptome survey reveals increased complexity of the alternative splicing landscape in Arabidopsis. *Genome Res.* **22**:1184–1195.

Marquez, Y., Höpfler, M., Ayatollahi, Z., Barta, A., and Kalyna, M. (2015). Unmasking alternative splicing inside protein-coding exons defines exitrons and their role in proteome plasticity. *Genome Res.* **25**:995–1007.

Martinière, A., Lavagi, I., Nageswaran, G., Rolfe, D. J., Maneta-Peyret, L., Luu, D.-T., Botchway, S. W., Webb, S. E. D., Mongrand, S., Maurel, C., et al. (2012). Cell wall constrains lateral diffusion of plant plasma-membrane proteins. *PNAS* **109**:12805–12810.

Mei, W., Boatwright, L., Feng, G., Schnable, J. C., and Barbazuk, W. B. (2017). Evolutionarily Conserved Alternative Splicing Across Monocots. *Genetics* **207**:465–480.

Men, S., Boutté, Y., Ikeda, Y., Li, X., Palme, K., Stierhof, Y.-D., Hartmann, M.-A., Moritz, T., and Grebe, M. (2008). Sterol-dependent endocytosis mediates post-cytokinetic acquisition of PIN2 auxin efflux carrier polarity. *Nat. Cell Biol.* **10**:237–244.

Müller, K., Hošek, P., Laňková, M., Vosolsobě, S., Malínská, K., Čarná, M., Fílová, M., Dobrev, P. I., Helusová, M., Hoyerová, K., et al. (2019). Transcription of specific auxin efflux and influx carriers drives auxin homeostasis in tobacco cells. *Plant J.* **100**:627–640.

Nakabayashi, K., Bartsch, M., Ding, J., and Soppe, W. J. J. (2015). Seed Dormancy in Arabidopsis Requires Self-Binding Ability of DOG1 Protein and the Presence of Multiple Isoforms Generated by Alternative Splicing. *PLOS Genetics* **11**:e1005737.

Nodzyński, T., Vanneste, S., Zwiewka, M., Pernisová, M., Hejátko, J., and Friml, J. (2016). Enquiry into the Topology of Plasma Membrane-Localized PIN Auxin Transport Components. *Molecular Plant* **9**:1504–1519.

O'Leary, N. A., Wright, M. W., Brister, J. R., Ciufo, S., Haddad, D., McVeigh, R., Rajput, B., Robbertse, B., Smith-White, B., Ako-Adjei, D., et al. (2016). Reference sequence (RefSeq) database at NCBI: current status, taxonomic expansion, and functional annotation. *Nucleic Acids Res.* **44**:D733-745.

Pernisova, M., Prat, T., Grones, P., Harustiakova, D., Matonohova, M., Spichal, L., Nodzynski, T., Friml, J., and Hejatko, J. (2016). Cytokinins influence root gravitropism via differential regulation of auxin transporter expression and localization in Arabidopsis. *New Phytologist* **212**:497–509.

Petrasek, J., Mravec, J., Bouchard, R., Blakeslee, J. J., Abas, M., Seifertová, D., Wisniewska, J., Tadele, Z., Kubes, M., Covanová, M., et al. (2006). PIN proteins perform a rate-limiting function in cellular auxin efflux. *Science* **312**:914–918.

Rademacher, E. H., and Offringa, R. (2012). Evolutionary Adaptations of Plant AGC Kinases: From Light Signaling to Cell Polarity Regulation. *Front. Plant Sci.* **3**.

Rakusová, H., Gallego‐Bartolomé, J., Vanstraelen, M., Robert, H. S., Alabadí, D., Blázquez, M. A., Benková, E., and Friml, J. (2011). Polarization of PIN3-dependent auxin transport for hypocotyl gravitropic response in Arabidopsis thaliana. *The Plant Journal* **67**:817–826.

Rakusová, H., Abbas, M., Han, H., Song, S., Robert, H. S., and Friml, J. (2016). Termination of Shoot Gravitropic Responses by Auxin Feedback on PIN3 Polarity. *Current Biology* **26**:3026–3032.

Reddy, A. S. N., Marquez, Y., Kalyna, M., and Barta, A. (2013). Complexity of the alternative splicing landscape in plants. *Plant Cell* **25**:3657–3683.

Remy, E., Cabrito, T. R., Baster, P., Batista, R. A., Teixeira, M. C., Friml, J., Sá-Correia, I., and Duque, P. (2013). A major facilitator superfamily transporter plays a dual role in polar auxin transport and drought stress tolerance in Arabidopsis. *Plant Cell* **25**:901–926.

Retzer, K., Butt, H., Korbei, B., and Luschnig, C. (2014). The far side of auxin signaling: fundamental cellular activities and their contribution to a defined growth response in plants. *Protoplasma* **251**:731–746.

Rosquete, M. R., von Wangenheim, D., Marhavý, P., Barbez, E., Stelzer, E. H. K., Benková, E., Maizel, A., and Kleine-Vehn, J. (2013). An Auxin Transport Mechanism Restricts Positive Orthogravitropism in Lateral Roots. *Current Biology* **23**:817–822.

Roychoudhry, S., Kieffer, M., Del Bianco, M., Liao, C.-Y., Weijers, D., and Kepinski, S. (2017). The developmental and environmental regulation of gravitropic setpoint angle in Arabidopsis and bean. *Sci Rep* **7**:42664.

Rueden, C. T., Schindelin, J., Hiner, M. C., DeZonia, B. E., Walter, A. E., Arena, E. T., and Eliceiri, K. W. (2017). ImageJ2: ImageJ for the next generation of scientific image data. *BMC Bioinformatics* **18**:529.

Ruzicka, K., Zhang, M., Campilho, A., Bodi, Z., Kashif, M., Saleh, M., Eeckhout, D., El-Showk, S., Li, H., Zhong, S., et al. (2017). Identification of Factors Required for m6A mRNA Methylation in Arabidopsis Reveals a Role for the Conserved E3 Ubiquitin Ligase HAKAI. *New Phytol* **215**:157–172.

Shang, X., Cao, Y., and Ma, L. (2017). Alternative Splicing in Plant Genes: A Means of Regulating the Environmental Fitness of Plants. *International Journal of Molecular Sciences* **18**:432.

Sibout, R., Sukumar, P., Hettiarachchi, C., Holm, M., Muday, G. K., and Hardtke, C. S. (2006). Opposite Root Growth Phenotypes of hy5 versus hy5 hyh Mutants Correlate with Increased Constitutive Auxin Signaling. *PLOS Genetics* **2**:e202.

Sievers, F., Wilm, A., Dineen, D., Gibson, T. J., Karplus, K., Li, W., Lopez, R., McWilliam, H., Remmert, M., Söding, J., et al. (2011). Fast, scalable generation of high‐quality protein multiple sequence alignments using Clustal Omega. *Molecular Systems Biology* **7**.

Soumpasis, D. M. (1983). Theoretical analysis of fluorescence photobleaching recovery experiments. *Biophysical Journal* **41**:95–97.

Sprague, B. L., and McNally, J. G. (2005). FRAP analysis of binding: proper and fitting. *Trends in Cell Biology* **15**:84–91.

Staiger, D., and Brown, J. W. S. (2013). Alternative splicing at the intersection of biological timing, development, and stress responses. *Plant Cell* **25**:3640–3656.

Stamm, S., Ben-Ari, S., Rafalska, I., Tang, Y., Zhang, Z., Toiber, D., Thanaraj, T. A., and Soreq, H. (2005). Function of alternative splicing. *Gene* **344**:1–20.

Swarup, K., Benková, E., Swarup, R., Casimiro, I., Péret, B., Yang, Y., Parry, G., Nielsen, E., De Smet, I., Vanneste, S., et al. (2008). The auxin influx carrier LAX3 promotes lateral root emergence. *Nat. Cell Biol.* **10**:946–954.

Szakonyi, D., and Duque, P. (2018). Alternative Splicing as a Regulator of Early Plant Development. *Front. Plant Sci.* **9**.

Tress, M. L., Abascal, F., and Valencia, A. (2017). Alternative Splicing May Not Be the Key to Proteome Complexity. *Trends in Biochemical Sciences* **42**:98–110.

Tseng, Q., Duchemin-Pelletier, E., Deshiere, A., Balland, M., Guillou, H., Filhol, O., and Théry, M. (2012). Spatial organization of the extracellular matrix regulates cell-cell junction positioning. *Proc. Natl. Acad. Sci. U.S.A.* **109**:1506–1511.

Tsugeki, R., Tanaka-Sato, N., Maruyama, N., Terada, S., Kojima, M., Sakakibara, H., and Okada, K. (2015). CLUMSY VEIN, the Arabidopsis DEAH-box Prp16 ortholog, is required for auxin-mediated development. *Plant J.* **81**:183–197.

Waldie, T., and Leyser, O. (2018). Cytokinin Targets Auxin Transport to Promote Shoot Branching. *Plant Physiol.* **177**:803–818.

Willige, B. C., Ahlers, S., Zourelidou, M., Barbosa, I. C. R., Demarsy, E., Trevisan, M., Davis, P. A., Roelfsema, M. R. G., Hangarter, R., Fankhauser, C., et al. (2013). D6PK AGCVIII Kinases Are Required for Auxin Transport and Phototropic Hypocotyl Bending in Arabidopsis. *Plant Cell* **25**:1674–1688.

Zadnikova, P., Petrášek, J., Marhavý, P., Raz, V., Vandenbussche, F., Ding, Z., Schwarzerová, K., Morita, M. T., Tasaka, M., Hejátko, J., et al. (2010). Role of PIN-mediated auxin efflux in apical hook development of Arabidopsis thaliana. *Development* **137**:607–617.

Zwiewka, M., Bilanovičová, V., Seifu, Y. W., and Nodzyński, T. (2019). The Nuts and Bolts of PIN Auxin Efflux Carriers. *Front Plant Sci* **10**.